land

MDPI

Article

Defining and Verifying New Local Climate Zones with Three-Dimensional Built Environments and Urban Metabolism

Siyeon Park, Sugie Lee * and Kyushik Oh

Department of Urban Planning and Engineering, Hanyang University, Seoul 04763, Republic of Korea; szyzzn@hanyang.ac.kr (S.P.); ksoh@hanyang.ac.kr (K.O.)
* Correspondence: sugielee@hanyang.ac.kr

Abstract: The urban heat island (UHI) effect, where the temperature in an urban area is higher than in the surrounding rural areas, is becoming a major concern. The concept of a Local Climate Zone (LCZ) system was devised to provide an objective framework for UHI research, which allows for a microscale definition of the UHI effect within urban areas by considering 'urban' and 'rural' as a continuum versus a dichotomy. However, most LCZ types are classified only by surface structure and coverings, which seem irrelevant to climatological and microscale concepts. In addition, microclimate is influenced by urban metabolism related to human activities as well as structural effects, but the LCZ-classification system does not incorporate these functional concepts. Therefore, this study proposes a novel urban-classification system that addresses the limitations of the LCZ concept by quantifying structural and functional elements of the city at the pedestrian level using S-DoT sensors and semantic segmentation techniques. This study holds significance as it suggests a New-LCZ (N-LCZ) system to support the classification framework of highly valid urban types and follow-up studies related to the UHI. Moreover, the N-LCZ offers a regional urban-planning strategy for sustainable development through a more valid classification system.

Keywords: urban heat island effect; local climate zones; urban microclimate; urban metabolism; semantic segmentation

Citation: Park, S.; Lee, S.; Oh, K. Defining and Verifying New Local Climate Zones with Three-Dimensional Built Environments and Urban Metabolism. *Land* **2024**, *13*, 1461. https://doi.org/10.3390/land13091461

Academic Editor: Nir Krakauer

Received: 26 July 2024
Revised: 2 September 2024
Accepted: 3 September 2024
Published: 9 September 2024

1. Introduction

Background

The urban heat island (UHI) effect, which refers to higher temperatures in urban areas compared to surrounding rural areas, is one of the most severe urban climate and environmental issues, occurring in various countries and regions worldwide [1]. As populations concentrate in urban areas due to urbanization and intense development, the intensity and frequency of UHIs are increasing [2]. With approximately 54% of the global population residing in urban areas today and an estimated increase to around 70% by 2050, the adverse effects of UHI are expected to worsen [3]. The ongoing influx of people and the rising levels of human activity contributing to urbanization in Seoul have led to numerous studies focusing on urban heat environments [4]. Increasing urbanization alters Seoul's thermal structure, making it particularly vulnerable to urban overheating, which makes it an ideal environment to examine the potential influence of meteorological factors on urban overheating [5]. Given the hot and humid conditions during the summer in Seoul, there is an urgent need for urban-planning strategies to address the UHI, which directly impacts the health of city residents.

In response to global climate change trends, the global application of the 'Köppen–Geiger Climate Zone Classification' has seen a resurgence for observing and predicting various climate zones [6]. As the urban heat island (UHI) phenomenon has become a significant urban issue, efforts to classify climate zones within cities have continued. Local Climate Zone (LCZ) system was introduced to standardize UHI observations globally and

provide an objective framework for UHI research [7]. They grouped areas with uniform surface structures, coverings, materials, and human activity characteristics at the horizontal scale to define LCZ types. These four categories of surface structure, cover, fabric, and human activity are variables determining urban factors influencing microclimate. Utilizing variables associated with these four categories, LCZs are categorized into 10 building types and 7 land-cover types. The LCZ maps generated simplify the representation of urban heat environment patterns according to defined LCZ classes, thereby supporting the development of urban planning and policies to address climate change [8]. Today, LCZ maps are applied in various studies, facilitating rapid assessment of temperature changes and helping to mitigate climate-related health issues [9,10].

LCZ was developed as a concept with regional and climatological characteristics in contrast to previous urban-classification systems; however, it still has limitations in terms of regional and climatological aspects, as follows. Firstly, temperature numerical modeling cannot accurately predict microclimates [7]. This assertion does not align with the original purpose of LCZ, which was created to identify regional UHIs within urban areas, as the boundaries between 'urban' and 'rural' are not clear in modern society. Secondly, LCZ classifies urban types focusing only on variables related to surface structure and cover. This narrow focus contradicts the LCZ's original purpose of overcoming the limitations of existing urban-classification systems, which lacked relevance to climate by selecting variables influencing microclimate.

Even so, the LCZ has been applied as a universal classification system for urban and natural landscapes in various urban-planning research domains up to the present [11,12]. Hence, this research aims to critically explore the LCZ concept and to devise a novel urban-classification framework, the New Local Climate Zones (N-LCZs), which encompass both regional and climatic significances by considering urban environmental and metabolic factors. Additionally, this study includes detailed case analyses comparing the statistical characteristics and actual spatial distribution characteristics of N-LCZ types and investigated the correlation between microclimate and N-LCZ to validate the effectiveness of N-LCZ.

2. Literature Review

2.1. Scale of Local Climate Zones

The scale of LCZs can be divided into two aspects: vertical and horizontal. Firstly, the vertical scale refers to the criterion height of temperature measurement in the LCZ original work [7]. LCZ uses screen air temperature as a reference, where the screen level represents a height of 1–2 m above the ground, similar to the pedestrian level. However, they pointed out in their original paper that the observation and numerical modeling techniques utilized for temperature investigation in LCZ types, which were being used in LCZ research, were not sufficiently developed to accurately predict microclimates at the screen level. Moreover, the original text does not explain to what vertical extent the variables used in microclimatic classification of LCZ types were quantified.

The horizontal scale of LCZs refers to the basic spatial unit, i.e., the analysis unit. Since the LCZ system literally represents local climate zones, the basic spatial unit should also be at a microscale. Additionally, each basic spatial unit should possess distinct urban environments differentiated from other spaces [8]. The conventional LCZ required a diameter ranging from a minimum of 400 m to a maximum of 1000 m to prevent overlap with surrounding types and to exhibit distinct characteristics [7]. However, basic spatial units with diverse areas may not represent a typical LCZ type [8].

2.2. Factors of Local Climate Zones

Urban attributes influencing temperatures at heights of 1–2 m above the ground were categorized into surface structure, cover, fabric, and human activity, with ten variables selected across these four categories [7]. Firstly, in terms of surface structure variables, Sky View Factor (SVF), aspect ratio, height of roughness elements, and terrain roughness class

were included. SVF refers to the amount of sky visible from the ground after excluding obstructions, and due to its strong correlation with urban heat environments, it is considered suitable for microscopically expressing the influence of urban morphology on heat environments [13]. Aspect ratio is defined as the ratio of the average height to width [14]. It plays an important role in managing urban microclimates as it alters the amount of solar radiation reaching a given surface and the flow of wind, and it is frequently used when investigating the correlation between urban geometry and urban microclimate [15]. The aspect ratio is defined by dividing it into three sub-elements: ratio of street canyons, ratio of building spacing, and ratio of tree spacing, based on LCZ types [7]. However, there is no unique formula for defining aspect ratio in complex urban geometries, and even in the original LCZ text, specific calculation formulas cannot be found [16]. Height of roughness elements is represented as building height for LCZ1 to LCZ10 built types and as tree height for LCZA to LCZG land-cover types [7]. However, urban forms, functions, and structural characteristics become increasingly complex and interconnected during urbanization [17], indicating that modern cities are not strictly classified into distinct built types and land-cover types. Thus, the criteria for determining height of roughness elements may not be clear, suggesting that the selection of building height or tree height may be inappropriate depending on the situation. Terrain roughness class is a variable indicating the degree of obstacles present on the surface, affecting wind speed and convection within urban canyons, thereby influencing UHI [18]. Terrain roughness is defined based on a previous classification of effective terrain roughness in both urban and rural landscapes [7,19]. However, this method only describes urban terrain roughness in eight types, limiting its applicability to high-density cities [20]. Therefore, it has been frequently excluded in previous studies utilizing the LCZ system [21,22].

Secondly, surface-cover variables include building surface fraction, pervious surface fraction, and impervious surface fraction. Building surface fraction refers to the proportion of the building footprint area within the basic spatial unit. Several studies have empirically demonstrated that building surface fraction is a factor influencing urban microclimate changes [23,24]. In particular, during the hot summer months when UHI effects are pronounced, a strong positive correlation between building surface fraction and temperature is observed compared to winter months [23]. In contrast, pervious areas including vegetation and water bodies are effective for urban cooling [25]. Cooling effects resulting from evapotranspiration within pervious areas have been empirically demonstrated in numerous previous studies, and their association with microclimate has been established, making them useful for UHI-mitigation strategies [26,27]. Additionally, a decrease in pervious surface fraction, resulting in a reduction in vegetation and water area, typically leads to an increase in impervious surface ratio, which alters the urban heat environment [28].

Thirdly, surface fabric variables include surface admittance and surface albedo. Surface admittance represents the capacity of a surface to absorb or emit heat locally, influencing surface heat accumulation and cooling rates [29]. However, there are minimal data available for measuring surface admittance at a microscopic scale [7], as it largely relies on subjective estimations. Due to the ambiguity in quantifying variables and limitations in data availability, surface admittance has frequently been excluded in LCZ-related studies [30,31]. Surface albedo refers to the ratio of solar radiation reflected by the surface to the solar radiation received by the surface. Numerous studies have empirically demonstrated urban temperature changes based on surface albedo conditions, and albedo mapping has been used to validate urban heat island patterns [32,33].

Fourthly, human activity variables include anthropogenic heat release. The average annual heat flux density was used as an indicator of anthropogenic heat release, which includes human activities such as fuel consumption, transportation, heating and cooling, industrial processes, and human metabolism [7]. However, their original paper does not include the calculation process or specific data descriptions for these variables. Moreover, UHI arises from complex interactions among factors such as building surface fraction, impervious surface ratio, albedo, and anthropogenic heat release [34]. Nonetheless, anthro-

pogenic heat release values in LCZ original texts exhibit consistent patterns of increase, decrease, or absence, indicating that the complex environmental attributes resulting from interactions among urban factors have not been adequately represented. Similarly, the utilization of anthropogenic activity variables is insufficient in numerous previous studies based on the LCZ system [35,36]. Overall, the LCZ system needs to be more closely associated with social indicators, such as human activities [37].

Nevertheless, considering anthropogenic heat in cities remains crucial, and anthropogenic heat release can be understood in the context of urban metabolism. 'Urban metabolism' represents the cyclical flow of resources and metabolic products, which are imported and exported through human activities such as fuel consumption, transportation, heating and cooling, industrial processes, and human metabolism, analogous to a living organism [38,39]. Anthropogenic heat release serves as an indicator of urban metabolism, quantifiable using factors such as population density, traffic volume, and energy consumption. Understanding urban metabolism has been facilitated by the flow of people and transportation, with population movement being the most influential factor in urban metabolism [40]. Consequently, areas with high human activity and traffic volume experience more severe heat impacts [41]. Moreover, from the perspectives of UHI and climate change, energy consumption is crucial for delineating urban metabolism [42]. In the case of the correlation between UHI intensity and energy usage, anthropogenic heat generated from energy consumption is a significant factor influencing urban thermal environments [43].

2.3. Research Gaps

Based on a review of previous studies, the limitations of LCZ can be summarized as follows. Firstly, while LCZ defines urban environmental factors influencing microclimate at the screen level and creates a classification system of urban types using related variables, the criteria for quantifying the vertical height of microclimate and urban environmental factors are unclear. Secondly, although LCZ should be defined at a microscopic scale, the minimum diameter range of 400–1000 m suggested in the original work lacks validity for claiming microscale representation and raises concerns about overlap with other spatial units. Thirdly, there is a lack of explanation regarding the definitions and specific formulas for the variables used, resulting in rare instances of complete reference to LCZ variables even in subsequent studies utilizing the LCZ framework. Lastly, despite the importance of urban metabolism, related indicators are not actively incorporated into LCZ classification, and regions defined without anthropogenic heat release values are considered inadequate reflections of the characteristics of modern cities.

To address these discrepancies, our study quantified urban microclimate and horizontal landscape factors at the screen level, similar to pedestrian height. Specifically, we measured microclimate using urban sensors installed within approximately 3 m above ground and derived the quantity of sky and greenery observed from the pedestrian perspective using street view images and semantic segmentation techniques. Furthermore, we utilized a semi-variogram model to determine basic spatial units that are microscopic yet not overlapping with other spaces. Additionally, the straightforward assimilation of our results in subsequent research is aided by including detailed definitions and formulas for variables used in the paper. Finally, by selecting population, traffic volume, and energy consumption as indicators of urban metabolism, we developed a new urban-classification system, N-LCZ, which encompasses both local and climatological factors.

3. Methodology

3.1. Research Scope

The spatial scope of this study is Seoul, the capital and largest city of South Korea (Figure 1). Located at 37° N latitude and 126° E longitude, Seoul experiences significant annual temperature variation, exhibiting characteristics of a humid continental climate in winter and hot, humid conditions in summer, which increase the risk of heat-related

illnesses. The total area of Seoul is approximately 605.21 km^2, with a registered population of around 9.66 million as of 2023. Given that urbanization leads to population concentration and increased building density, contributing to the UHI effect, Seoul, as one of the most densely populated cities globally, is a region where UHI management is crucial. The temporal scope of this study includes the summer period, when the UHI impact is most pronounced, specifically from 1 June to 31 August 2021.

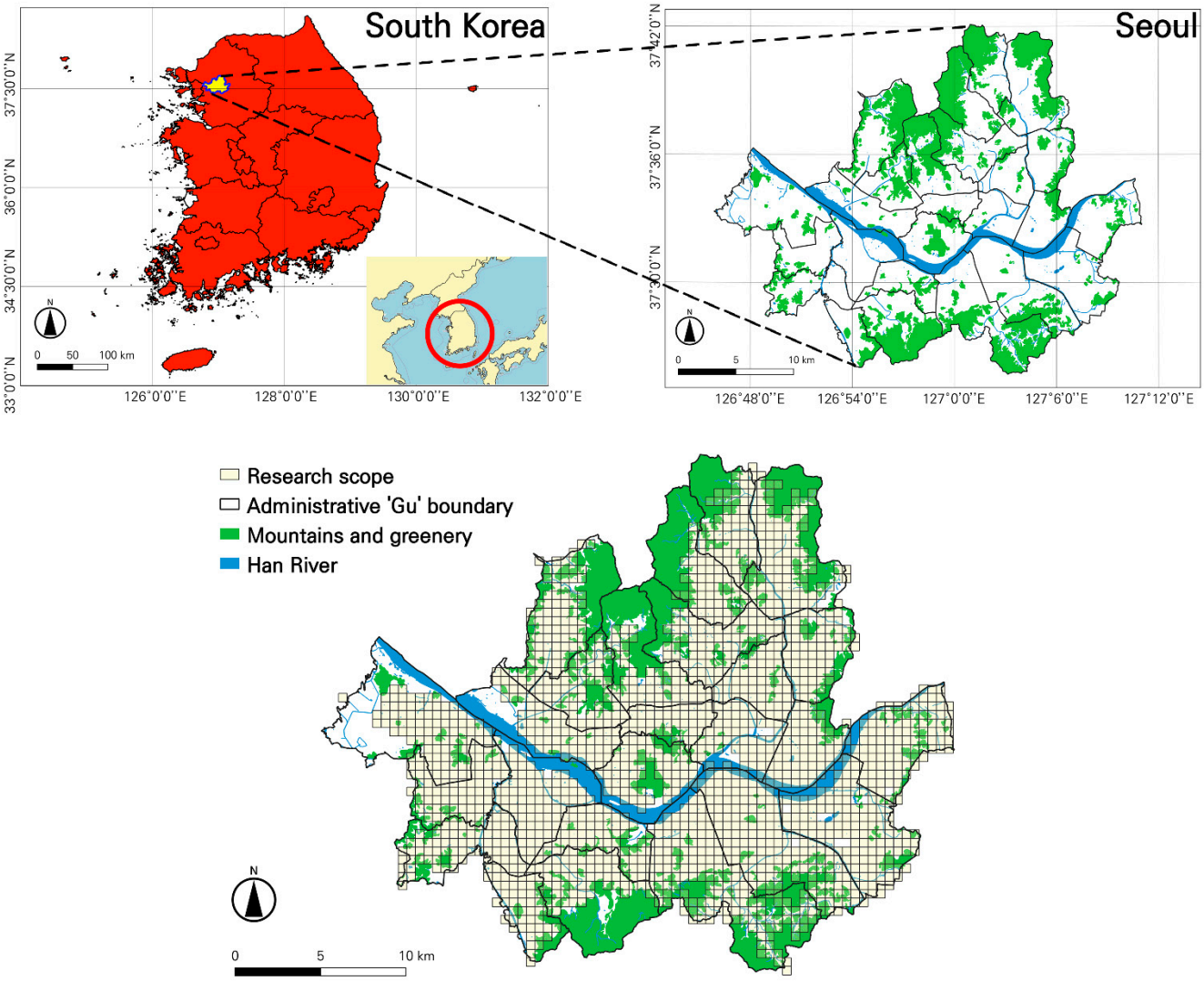

Figure 1. Location map of the study area.

The analytical unit of this study, set against the backdrop of Seoul, consisted of grid cells measuring 500 m × 500 m. To establish a consistent scale for defining urban typology, this study adopted regular grids as the basic spatial unit [44]. Determination of the size of these regular grids relied on the spatial autocorrelation of building height [35,45]. Within areas exhibiting a uniform urban form, there exists spatial autocorrelation of building height [45], making it suitable for identifying regions with uniform spatial attributes and defining N-LCZ in this study. Through the analysis depicted in Figure 2, this study confirmed that building height exhibits spatial autocorrelation when the distance between buildings in Seoul is approximately 423 m or less. Consequently, grid cells measuring 500 m × 500 m were chosen as the analytical unit for this study. However, of the 2633 orthogonal grids created based on the boundaries of Seoul, 743 grids where urban environmental factor variables utilized in this study were not collected were excluded from the analysis. As a result, the study was conducted on 1890 grid cells.

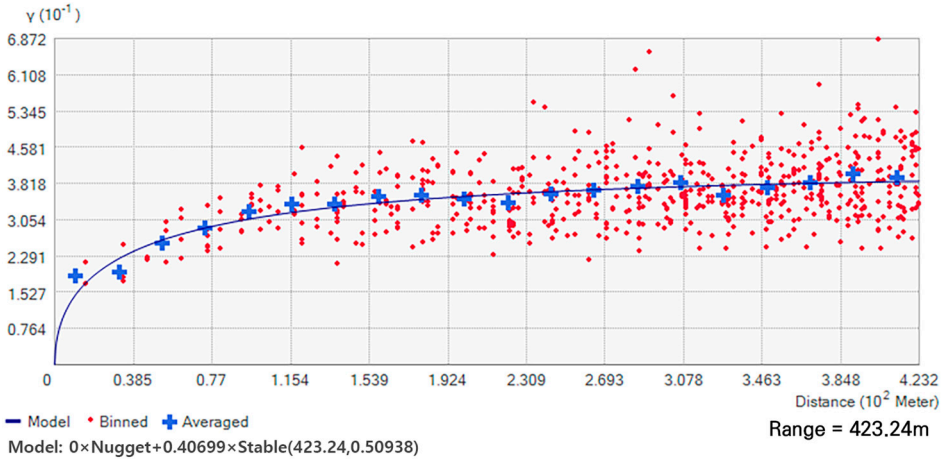

Figure 2. Semi-variogram (spatial autocorrelation of building heights in Seoul).

3.2. Data Collection

To analyze whether LCZ and N-LCZ correlate with microclimate, we initially utilized urban sensors named Smart Seoul Data of Things (S-DoT) to survey the microclimate in Seoul. S-DoT sensors are predominantly installed around 3 m above ground, such as on streetlights and CCTV, thus measuring urban microclimate at closely resembling pedestrian-level conditions [46]. Furthermore, as of 2023, approximately 1100 sensors had been deployed across Seoul, indicating a denser distribution compared to traditional ground observation methods like Automatic Weather Stations.; thus, utilizing S-DoT sensors allows for a microscale analysis both vertically and horizontally. Therefore, the S-DoT network is an effective tool for monitoring temperatures within new 'Local' Climate Zones and is specifically designed to collect data in Seoul, South Korea. The spatial distribution and installation examples of these sensors within the city are presented in Figure 3. Information on the sensor resolution and temperature data used in this study is detailed in Table 1. We applied kriging interpolation at S-DoT locations to generate spatially continuous temperature distribution maps. Additionally, we calculated the average air temperature within each analysis unit.

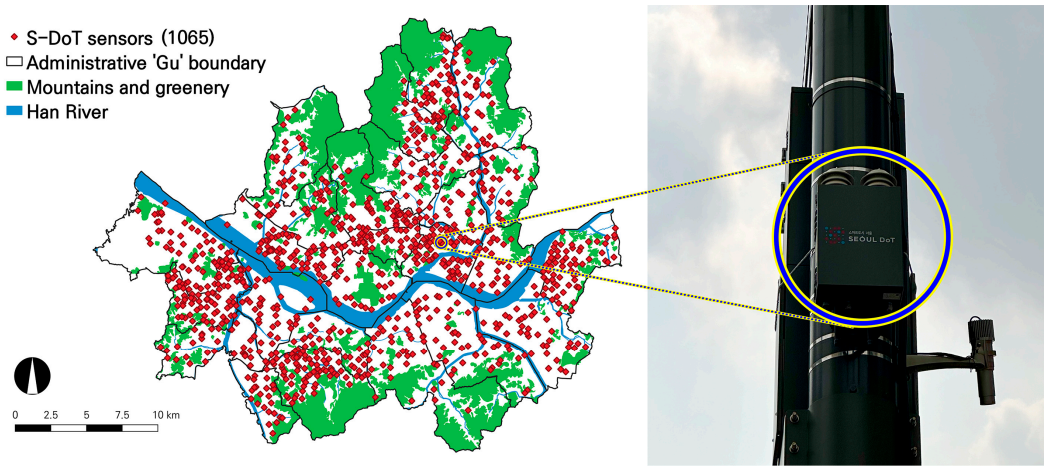

Figure 3. The spatial distribution and examples of installations of S-DoT.

This study investigated the spatial distribution of LCZ types in Seoul using the database provided by the World Urban Database and Access Portal Tools (WUDAPT). The WUDAPT program, offering automated quality control through cross-validation between training and test areas, is deemed reliable for LCZ classification in urban settings [47]. We selected the Seoul LCZ database generated in April 2021. Since the program's LCZ

map is available at a 100 m resolution, we re-mapped it onto a grid size of 500 m × 500 m, consistent with the analysis unit of this study, to facilitate the comparative analysis with N-LCZ. Using GIS, we identified the predominant LCZ type within each basic spatial unit, and defined it as the LCZ type at a 500 m resolution, thereby creating the final LCZ map of Seoul.

Table 1. Details of the S-DoT sensors used in the study.

Smart Seoul Data of Things (S-Dot) Sensors	**Spatial Resolution**	1065 Stations
	Temporal Resolution	One Hour
	Usage	Air Temperature
Year		2021
Acquisition date		6/1–8/31 (total 92 days)

The definitions and sources of the variables utilized for development of N-LCZ are as presented in Table 2. The N-LCZ variables were selected based on the literature review outlined in Chapter 2, categorizing all variables into urban environmental factors and urban metabolic factors. Urban environmental factors encompass variables related to surface structure, cover, and fabric as discussed in the original LCZ paper, while urban metabolic factors are associated with human activity variables from the original text.

Table 2. Description of variables.

Variables			**Description**	**Sources**
Microclimate		Air temperature (°C)	The average air temperature in the analysis unit *	Seoul Open Data Plaza (2021)
Urban environmental factors	Surface structure	SVF (%)	The proportion of sky measured at the pedestrian level within the analysis unit	Naver Street View (2021)
		GVF (%)	The proportion of greenery measured at the pedestrian level within the analysis unit	
		Aspect ratio	The ratio of average building height to average road width within the analysis unit	New address Database (2021)
		DEM (m)	The average elevation within the analysis unit	V-World (2021)
		Building height (m)	The average building height within the analysis unit	New address Database (2021)
		Surface roughness (m)	The standard deviation of the sum of elevation and building height within the analysis unit	New address Database (2021)/V-World (2015)
	Surface cover	Building surface fraction	The proportion of total building floor area within the analysis unit	New address Database (2021)/V-World (2021)
		Pervious surface fraction	The proportion of total impervious surface area (including vegetation and water bodies) within the analysis unit	
		Impervious surface fraction	The proportion of area excluding building surfaces and impervious surfaces within the analysis unit	
	Surface fabric	Surface albedo	The proportion of average solar irradiance reflected within the analysis unit	Landsat8

Table 2. *Cont.*

Variables			Description	Sources
Urban metabolic factors	Human activity	Population density (people/m^2)	Total residential population per analysis unit	Seoul Open Data Plaza (2021)
		Traffic volume	The normalized index of total estimated traffic volume within the analysis unit	View-T (2021)
		Electricity energy consumption (kWh/m^2)	Total electricity consumption per analysis unit	Architecture Data Private Opening System (2021)

* Grid of 500 m × 500 m.

In this study, Naver Street View (NSV) and semantic segmentation techniques were combined to quantify Sky View Factor (SVF) and Green View Factor (GVF). NSV provides panoramic big datasets along road networks, while semantic segmentation is a computer vision technique for efficiently processing large-scale image data, such as street view images. The aim of this research was to overcome limitations of outdated LCZ theory and to develop a new urban typology-classification system that encompasses both local and climatological significance. Therefore, the variables used in N-LCZ development needed to be measured microscopically from both vertical and horizontal perspectives. Existing remote sensing-based technologies have limitations in extracting street-level urban landscapes. However, street view images provide data at pedestrian levels, thereby overcoming this limitation and offering the advantage of more realistically reflecting the current situation of street canyons [48,49].

We generated points at 50 m intervals based on road network data from 2021, which served as the temporal background of our study, and collected NSV panoramic images for each point. Next, we applied semantic segmentation techniques to NSV panoramic images to identify horizontal landscape elements. To represent the three-dimensional horizontal landscape, panoramic images processed through semantic segmentation were corrected into a fisheye perspective [49]. Fisheye images like Figure 4 were generated, where the ratio of sky object pixels to the total number of pixels within the image was defined as SVF, and the ratio of green object to total pixels was defined as GVF. This study aggregated the mean values of SVF and GVF within a 500 m × 500 m grid as variables. However, out of 2633 grids generated for Seoul, 743 grids lacked data on SVF and GVF and were thus excluded from the study. Ultimately, the study focused on 1890 grids.

In the LCZ theory, criteria for aspect ratio, height of roughness elements, and terrain roughness class were ambiguous. Concerning aspect ratio, although it was delineated into three sub-concepts—ratio of street canyons, ratio of building spacing, and ratio of tree spacing—based on built types and land-cover types, the structural and functional characteristics of modern cities are interconnected, suggesting the possibility that they may not be fully classified into distinct built and land-cover types [17]. Therefore, to represent the complex geometric structures of Seoul's streets, where building heights and road widths vary within a single street, we measured the aspect ratio using a street canyon ratio, calculated by dividing the average building height by the average road width [45].

The height of roughness elements in this study was calculated based on building height. Originally, the height of roughness elements, like aspect ratio, was a variable based on building height and tree height according to LCZ's built and land-cover types. Modifying the criteria based on building height or tree height depending on the surrounding environment, similar to aspect ratio, implies potential ambiguity in classification results. This study considered building factors to be important in densely populated modern cities and thus determined the height of roughness elements focusing on building height in line with numerous LCZ-related studies [50,51].

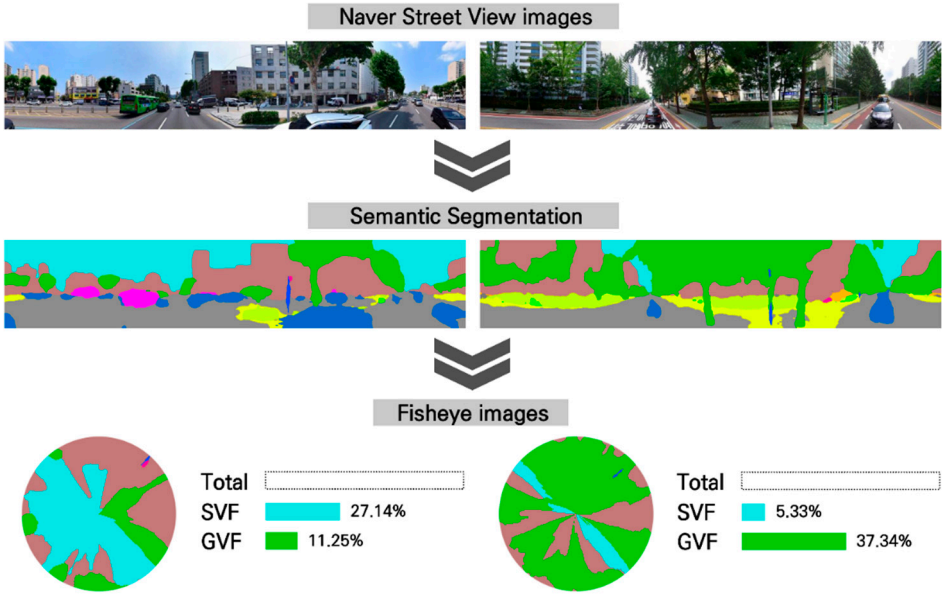

Figure 4. Example of Naver Street View image and semantic segmentation.

The terrain roughness class [19], as employed in the LCZ original text, is not suitable for application in modern high-density cities; therefore, terrain roughness class has often been excluded in subsequent LCZ studies [20–22]. In this study, considering buildings as the main features of urban surfaces, terrain roughness was defined by referencing a study that quantifies it through the variation in height of elevation and buildings [52]. In Korea, various large and small hills exist within cities, potentially affecting surface roughness; thus, this study defines terrain roughness class by considering both elevation and building height, not just building height alone. Ultimately, we have termed the terrain roughness class as surface roughness.

3.3. Analysis Method

The aim of this study is to propose N-LCZ by grouping areas with similar attributes within the analysis units. We validate the viability of N-LCZ through descriptive statistical analysis, spatial distribution analysis, and correlation analysis, demonstrating its distinct advantages over the existing LCZ (Figure 5). Initially, hierarchical clustering was employed to define N-LCZ. Agglomerative hierarchical clustering has been the dominant approach to constructing embedded classification schemes [53]. Compared with other classic clustering algorithms, agglomerative hierarchical clustering algorithms have higher time complexity and space complexity, but generally do not require determining initial partitions and do not generate noise points [54]. Agglomerative hierarchical clustering groups clusters based on the distance between them. The distance between clusters is typically defined using single, complete, average, centroid, or Ward linkage methods. Among them, the Ward linkage method focuses on merging data based on the sum of squares of deviations within clusters rather than simply the distance between clusters, making it less sensitive to noise or outliers [55]. Therefore, this study employed agglomerative hierarchical clustering using the Ward linkage method in Python and defined an N-LCZ type with similar properties.

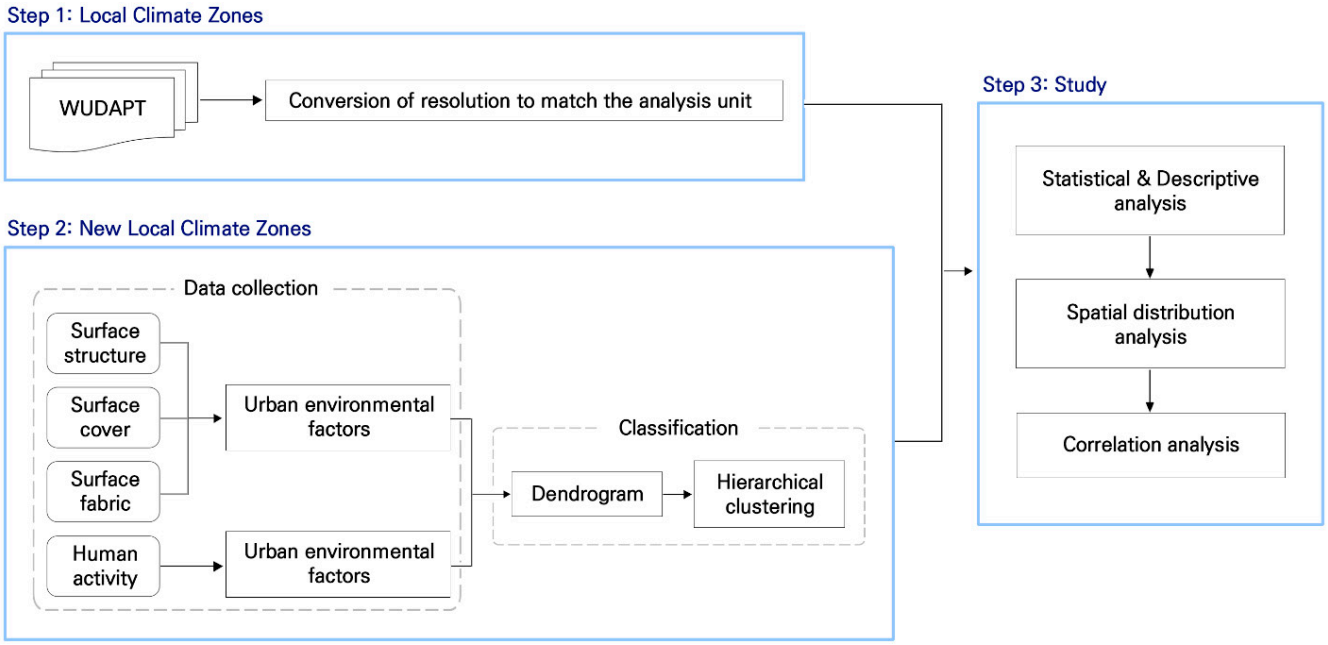

Figure 5. Overall methodology flowchart of this study.

Next, to visualize the process of attributes combining for the basic spatial units created earlier, we constructed a dendrogram graph. The height of the dendrogram is proportional to the average distance within the clusters, and the horizontal width is proportional to the number of data points included in the clusters [56]. An increase in the average distance within clusters implies a decrease in similarity among objects within the clusters, indicating that the similarity of objects constituting the clusters is inversely proportional to the height of the dendrogram. Therefore, in this study, we determined the optimal number of clusters (k) to ensure that the similarity among clusters is not significantly different, i.e., the deviation in cluster heights is not large. We confirmed that similar height clusters were formed when k was 12, thus selecting 12 as the optimal number of urban types for defining N-LCZ.

4. Results

4.1. Critical Research on Local Climate Zones

Figure 6 depicts the LCZ map of Seoul, classified into 500 m × 500 m grid resolutions using the WUDAPT program. Additionally, we verified the actual distribution areas of the LCZ types using NSV images and compared the characteristics and spatial distribution of these types (Figure 6). We discovered discrepancies between the defined characteristics and the spatial distribution of each LCZ type. Firstly, LCZ1 (Compact/high-rise) typifies areas with dense high-rise buildings and is predominantly observed in districts like Gangnam-gu, Seocho-gu, Jung-gu, Yeongdeungpo-gu, and Geumcheon-gu. However, parts of Gangnam-gu such as Yeoksam-dong feature many low-rise buildings, suggesting that some areas classified as LCZ1 do not distinctly exhibit high-rise characteristics. Secondly, LCZ2 (Compact/mid-rise) is characterized by areas with a dense concentration of mid-rise buildings. In Seoul, this type is predominantly observed in the districts of Seodaemun-gu, Gwanak-gu, Dongjak-gu, and Seongbuk-gu. However, regions like Bukahyeon-dong and Hongje-dong in Seodaemun-gu consist of relatively low-rise buildings, leading to a mismatch between the actual spatial distribution and LCZ2 characteristics. Thirdly, from LCZ4 (Open/high-rise) to LCZ6 (Open/low-rise), types are defined by low building density. These types are seen in areas like Bangi-dong and Garak-dong in Songpa-gu, Jamwon-dong and Banpo-dong in Seocho-gu, and Mok-dong and Sinjeong-dong in Yangcheon-gu. However, these regions are characterized by high building density and dense apartment cYeokomplexes, which do not align with the defined characteristics of LCZ4 to LCZ6.

Fourthly, LCZA-G (land-cover types) implies areas devoid of human activity. However, this type was found in bustling areas such as around Gimpo Airport in Gangseo-gu, Yeouido Hangang Park in Yeongdeungpo-gu, and Jamsil Hangang Park in Songpa-gu, suggesting further inconsistencies between LCZ type characteristics and their spatial distribution. Details of the spatial distribution of LCZ types in Seoul and the number of grids each type occupies are introduced in Appendix A.

Figure 6. The LCZ map of Seoul and examples of actual distribution areas by type.

To analyze the correlation between Seoul's LCZ types and microclimates, we rearranged the numbering of LCZ types from those generally considered to have higher temperatures to those considered to have lower temperatures, based on previous studies on the relationship between LCZ and temperature. We referred to the study, which investigated the suitability of the LCZ concept for UHI research by analyzing temperatures of LCZ types in 50 cities worldwide [57]. Additionally, we supplemented this survey with the research, which analyzed the relationship between LCZ types and summer temper-

atures [58]. Through this rearrangement process, as depicted in Figure 7, we found that LCZA is the lowest summer temperature type and LCZ2 is the highest summer temperature type. From this analysis, we observed a correlation coefficient of approximately 0.27 between LCZ type and microclimate, indicating a weak correlation between them. This result contradicts the goal of LCZ theory to create a system for classifying urban types based on local and climatological characteristics, suggesting that the term 'local climate zones' may not be appropriate.

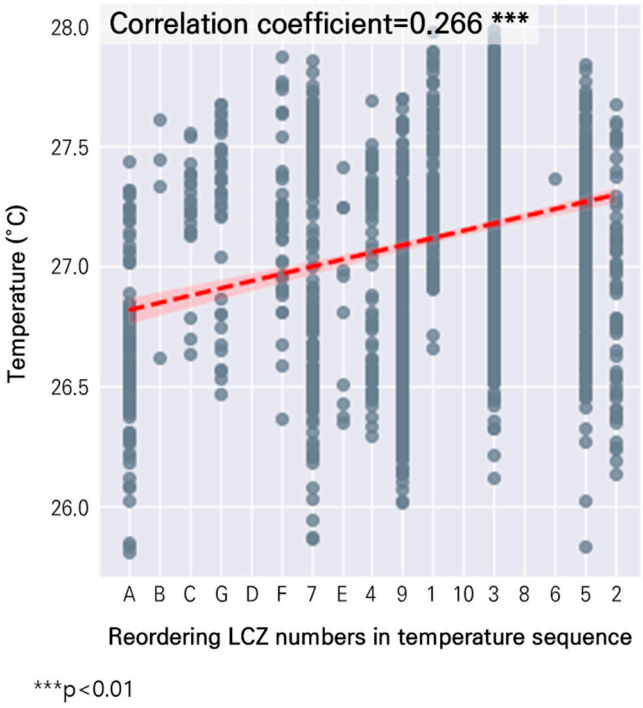

Figure 7. Correlation analysis between local climate zones and microclimate.

4.2. New Local Climate Zone System Development

To establish the concept of N-LCZ, we quantified urban environmental factors including SVF, GVF, aspect ratio, Digital Elevation Model (DEM), building height, surface roughness, building surface fraction, pervious surface fraction, impervious surface fraction, surface albedo, and urban metabolic factors that include population density, traffic volume, and electricity energy consumption. The statistical analysis results are shown in Table 3. The average air temperature during the summer of 2021 was recorded as 27.12 degrees Celsius. The proportions of visible sky and greenery, namely SVF and GVF, were calculated to be approximately 18.78% and 13.80%, respectively. The average aspect ratio was 0.63, the average DEM was 36.31 m, the average building height was 12.60 m, and the average surface roughness was 12.70 m. Surface-cover variables, including building surface fraction, pervious surface fraction, and impervious surface fraction, were derived as averages of 0.21, 0.17, and 0.63, respectively, indicating that Seoul has over three times more impervious surface cover compared to pervious surface cover. Among urban metabolic factors, the average population density was 0.5 individuals per square meter, the normalized average traffic volume was 0.2, and the average electricity energy consumption was 0.38 kWh per square meter.

We previously determined the optimal number of urban types for the N-LCZ system to be 12 using dendrogram. The attribute values of the defined 12 types are illustrated in Figure 8, where the values are categorized into three levels from minimum to maximum. The upper values are represented in red, the median values in yellow, and the lower values in blue. Furthermore, to intuitively grasp the key variables of each N-LCZ type, we normalized the attributes of the types and created a radar chart (Figure 9). Using the

attribute values shown in Figures 8 and 9, the names of the N-LCZ types were defined. The final definitions and spatial distribution map for the N-LCZ types are displayed in Figure 10. Descriptions of the spatial distribution characteristics for each type are as follows, and the spatial distribution maps by type are presented in Appendix B.

Table 3. Descriptive statistics of urban environmental and metabolic factors.

Variables			Obs.	Mean	Std. Dev.	Min.	Max.
		Air temperature (°C)	1890	27.12	0.44	25.81	27.98
Urban environmental factors	Surface structure	SVF (%)	1890	18.78	7.91	0.17	59.48
		GVF (%)	1890	13.80	10.44	0.00	66.88
		Aspect ratio	1890	0.63	0.41	0.00	10.18
		DEM (m)	1890	36.31	29.03	4.05	266.48
		Building height (m)	1890	12.60	9.49	0.00	150.00
		Surface roughness (m)	1890	12.70	7.41	0.00	62.91
	Surface cover	Building surface fraction	1890	0.21	0.13	0.00	0.52
		Pervious surface fraction	1890	0.16	0.24	0.00	1.00
		Impervious surface fraction	1890	0.63	0.20	0.00	1.00
	Surface fabric	Surface albedo	1890	0.60	0.08	0.28	0.94
Urban metabolic factors	Human activity	Population density (people/m^2)	1890	0.50	0.33	0.00	3.97
		Traffic volume	1890	0.20	0.13	0.00	1.00
		Electricity energy consumption (kWh/m^2)	1890	0.38	1.41	0.00	35.03

N-LCZ	n	AT	SVF	GVF	AR	DEM	BH	SR	BSF	PSF	ISF	SAL	PD	TV	EN
1	369	27.27	16.58	10.46	0.64	23.22	12.34	12.43	0.26	0.04	0.70	0.62	0.63	0.20	0.57
2	108	27.14	15.88	29.59	0.82	21.65	24.72	21.75	0.14	0.06	0.80	0.59	0.58	0.20	1.07
3	445	27.31	14.80	6.34	0.69	30.76	9.62	9.50	0.37	0.03	0.60	0.58	0.76	0.22	0.10
4	179	26.90	27.17	15.24	0.62	26.16	18.71	15.03	0.09	0.09	0.82	0.65	0.27	0.13	0.48
5	174	27.05	19.08	16.25	0.56	37.00	13.62	15.06	0.15	0.14	0.72	0.58	0.37	0.18	0.43
6	117	26.78	21.68	22.45	0.59	64.67	14.76	16.44	0.09	0.42	0.50	0.61	0.24	0.14	0.39
7	62	26.61	14.19	41.44	0.63	98.54	9.96	10.69	0.03	0.82	0.15	0.62	0.10	0.08	0.28
8	130	27.40	15.58	9.07	0.71	28.31	12.13	14.11	0.28	0.05	0.67	0.58	0.77	0.47	0.31
9	27	27.35	39.69	13.51	0.39	7.74	12.49	6.44	0.01	0.78	0.21	0.38	0.15	0.24	0.21
10	97	27.06	15.67	11.06	0.66	46.08	9.50	12.66	0.22	0.34	0.45	0.58	0.41	0.19	0.19
11	101	26.93	20.09	12.31	0.59	75.82	8.88	12.89	0.08	0.70	0.22	0.60	0.17	0.16	0.25
12	81	26.61	34.98	19.69	0.24	39.66	6.25	5.06	0.03	0.06	0.91	0.67	0.07	0.07	0.42

AT	Air temperature	BH	Building height	SAL	Surface albedo
SVF	Sky view factor	SR	Surface roughness	PD	Population density
GVF	Green view factor	BSF	Building surface fraction	TV	Traffic volumne
AR	Aspect ratio	PSF	Pervious surface fraction	EN	Electricity energy consumption
DEM	Digital elevation model	ISF	Impervious surface fraction		

Figure 8. Attributes of new local climate zones by type.

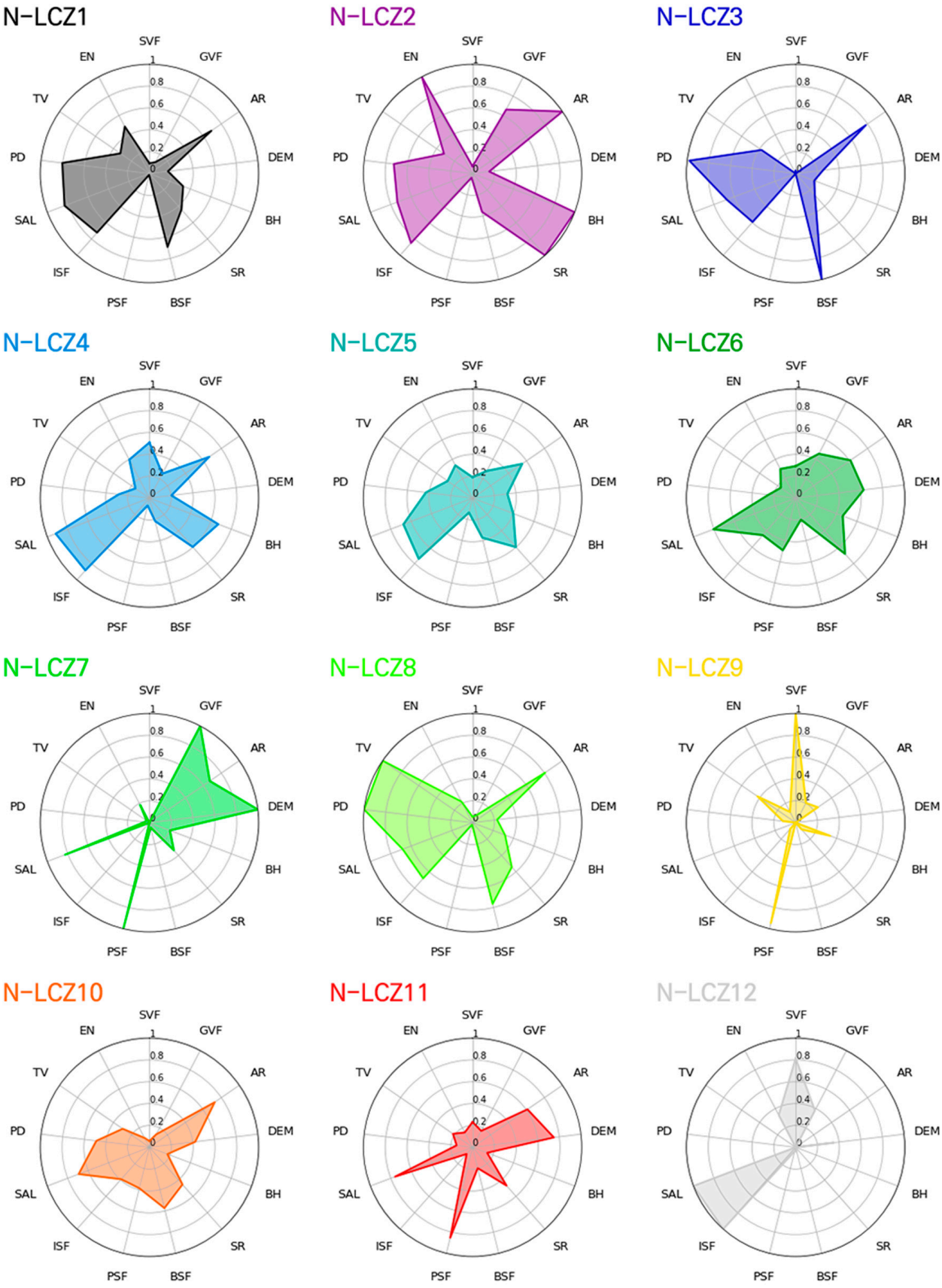

Figure 9. Radar chart of new local climate zones by type.

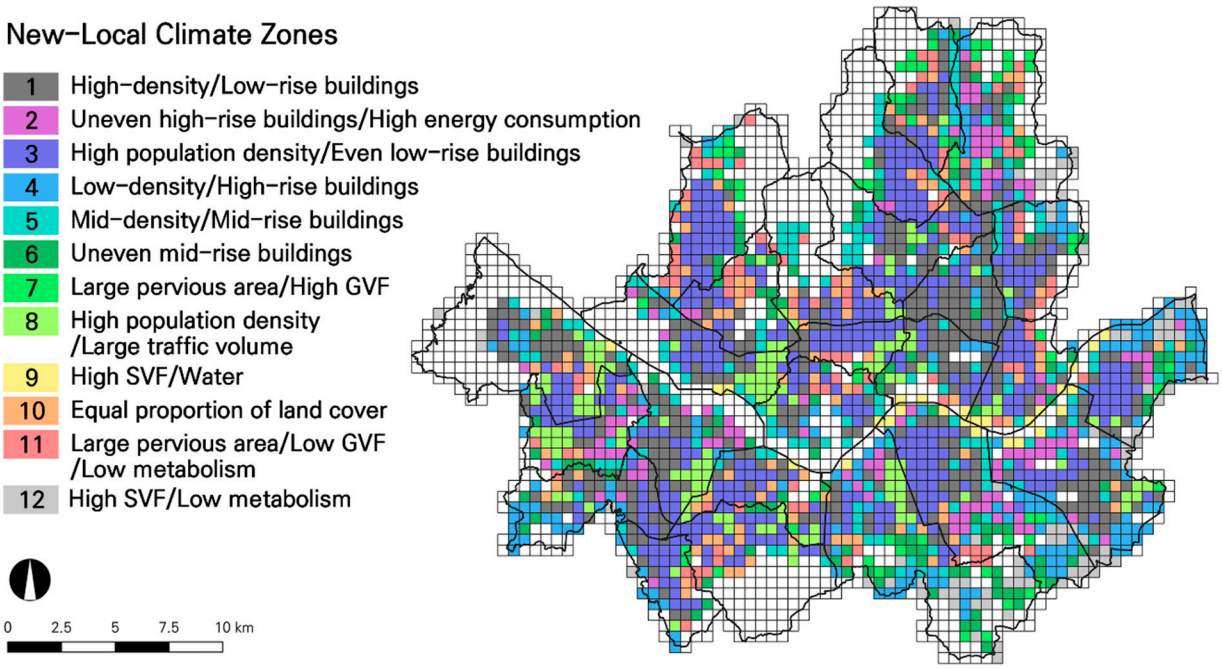

Figure 10. Spatial distribution of new local climate zones in Seoul.

N-LCZ1 is defined by a high building density and a predominance of low-rise buildings, leading to its designation as 'High-density/Low-rise buildings'. This type is also characterized by a high percentage of impervious surfaces and a dense population. The number of grids occupied by N-LCZ1 was 369, representing the second-largest area within Seoul. This type was primarily observed in concentrated clusters in Dongdaemun-gu and Seongdong-gu. Additionally, clusters of N-LCZ1 were observed in some areas of Gangseo-gu, Yeongdeungpo-gu, Geumcheon-gu, and Songpa-gu. These areas were found to have a high density of mid-rise apartment complexes or residential areas; thus, the spatial characteristics of N-LCZ1 align with the statistical characteristics of N-LCZ1. Furthermore, the classification reliability of the results was deemed high as the Seoul Asan Medical Center (sixth) in Songpa-gu and the Seoul Agricultural and Fisheries Marketing Corporation (tenth) in Songpa-gu, designated as energy-intensive buildings in 2021, are defined as N-LCZ1 with high-electricity-energy-consumption attributes.

N-LCZ2, compared to N-LCZ1, does not have a high building density but is characterized by having the tallest buildings among all types. Due to the large standard deviation in building height, it has been defined as 'Uneven High-rise Buildings'. Additionally, as this type exhibits the highest electricity consumption, it is also labeled 'high energy consumption'. The number of grids corresponding to N-LCZ2 was 108. This type was found in riverside apartment complexes in Seocho-gu, Gangnam-gu, and Songpa-gu, with riverside apartment complexes also identified in Gangnam-gu around the Yangjaecheon stream. Additionally, large apartment complexes in Mok-dong and Yangcheon-gu, were classified as N-LCZ2, and clusters of N-LCZ2 identified in Gangdong-gu and Nowon-gu were also apartment complexes. Given that these areas mainly consisted of apartment complexes, it can be inferred that they have high average building heights and significant height differences compared to buildings outside the complexes. Therefore, the spatial characteristics of N-LCZ2 align with its statistical characteristics, which include high building heights and surface roughness. Additionally, the inclusion of KT Mok-dong Internet Data Center (third) in Yangcheon-gu and Samsung Seoul Hospital (seventh) in Gangnam-gu in N-LCZ2 further confirms the clear characteristic of high electricity consumption in this type.

N-LCZ3 is defined by the highest building density among all types, yet features low-rise buildings in comparison. Additionally, this type is characterized by a very high population density, leading to its designation as 'high population density/even low-rise

buildings'. N-LCZ3 encompassed the highest number of grids, totaling 445, and its average temperature also ranked among the top 3 types. Representative areas included Sinsa-dong, Nonhyeon-dong, and Yeoksam-dong in Gangnam-gu, around Seokchon Lake in Songpa-gu, and Myeong-dong and Euljiro in Jung-gu. These areas are densely populated with buildings and experience high population mobility, aligning spatially with the attributes of N-LCZ3, characterized by high building surface fraction, population density, and traffic volume. Additionally, Sillim-dong in Gwanak-gu, Sangdo-dong and Noryangjin in Dongjak-gu, Hwagok-dong in Gangseo-gu, and the entire Eunpyeong-gu have been classified as N-LCZ3. These areas all feature densely arranged low-rise buildings. Therefore, it is concluded that the defined attributes and spatial distribution of N-LCZ3 are consistent.

N-LCZ4 is defined as 'Low-density/High-rise buildings' due to its low building surface ratio and high building heights. Additionally, this type is characterized by a high proportion of impervious surfaces. In practice, this type is typically found in areas with low-density apartment complexes and major roads. Notable areas include the outskirts of Guro-gu, Geumcheon-gu, Gangdong-gu, and the regions around Olympic-daero in Seocho-gu. These regions display the distinct features of N-LCZ4, with high building heights, low building density, and significant impervious surfaces from roads. N-LCZ4 encompasses 179 grids, making it the third largest area among all types.

N-LCZ6 is defined as 'Uneven Mid-rise Buildings' due to its large standard deviation in building heights and the predominance of medium-height buildings. Unlike most types, this classification generally represents relatively higher altitudes. Typically, N-LCZ6 is primarily found near Bukhansan in Jongno-gu, Seodaemun-gu, and Eunpyeong-gu; around Umyeon Mountain in Seocho-gu; and near Daemo Mountain and Guryong Mountain in Gangnam-gu. While primarily distributed along mountainous regions, N-LCZ6 is predominantly observed in areas close to the mountains, typically where buildings are also present. This characteristic reflects the N-LCZ6 properties of having mid-range building heights in higher-altitude areas. Statistically, the similarity in the proportions of permeable and impermeable surfaces is consistent with the spatial distribution features.

N-LCZ7 is named 'large pervious area/high GVF' due to its characteristics of having the highest pervious surface ratio, GVF, and altitude. This type is typically found in major mountainous areas such as Umyeon Mountain, Namsan, Achasan, and Bukhansan. Being centered in mountainous regions, N-LCZ7 statistically shows the highest pervious surface ratio, GVF, and altitude, aligning well with its geographical distribution. In contrast to N-LCZ6, which is observed in the urban areas at the base of mountains, N-LCZ7 is found in the central mountain areas, reflecting its high GVF and pervious surface ratio.

N-LCZ8 is named 'high population density/large traffic volume' due to its significantly higher population density and traffic volume compared to other types. N-LCZ8 covered 130 grids and was characterized by the highest average temperature. Spatially, N-LCZ8 was clustered in areas such as Ahyeon-dong, Gongdeok-dong, and Dohwa-dong in Mapo-gu, Sindang-dong in Jung-gu, and Singil-dong in Yeongdeungpo-gu. Additionally, areas along the Gyeongbu Expressway from Banpo IC to Seocho IC were classified as N-LCZ8. Residential areas densely packed with housing and areas including Sinwol IC in Yangcheon-gu were also classified as N-LCZ8. These areas distinctly reflect the attributes of N-LCZ8, which ranks second in building surface ratio and experiences the highest population density and traffic volume among all types.

N-LCZ9 exhibited a distinct spatial characteristic, primarily located around the Han River. N-LCZ9 has a very high SVF and is located in the area around the Han River, which gives it a distinct spatial characteristic. Therefore, we have defined it as 'high SVF/water'. In particular, only grids where NSV were collected were considered in this study's spatial scope. The grids where NSV was collected by traversing the Han River by car would include the major bridges over the river. Therefore, the classification of areas along the Han River as N-LCZ9, which has a very high impervious surface ratio but the second-highest traffic volume, is considered a highly reliable result.

N-LCZ11 is characterized by a relatively high proportion of pervious area and a very low GVF compared to other types. Additionally, urban metabolism variables such as population density, traffic volume, and electricity consumption are all lower for this type compared to others. Therefore, we have defined this type as 'Large pervious area/Low GVF/Low metabolism'. N-LCZ11 was situated around mountains such as Mt. Bukhan, Mt. Nam, Mt. Gwanak, and Mt. Guryong. Additionally, it included downtown parks in Seongdong-gu, Nowon-gu, and Yang-cheon-gu. Similar to N-LCZ7, N-LCZ11 is characterized by a high pervious surface fraction, but unlike N-LCZ7, which has the highest GVF, N-LCZ11 has a relatively lower GVF.

N-LCZ12 is characterized by a very high SVF and a high proportion of pervious surfaces, while it is defined as having very low urban metabolism factors, particularly population density and traffic volume. Therefore, we have named this type 'high SVF/low metabolism'. N-LCZ12 was concentrated in the outskirts of urban areas in Seocho-gu, Gangnam-gu, Gangdong-gu, and Nowon-gu, particularly in areas with nearby mountains and major roads. Given their location in the outskirts of the city, there may not be many buildings, but a high proportion of impervious surfaces such as roads has been observed. Additionally, the spatial characteristics of the outer areas with low population density and traffic volume reflect the statistical characteristics of N-LCZ12.

The geographic information system (GIS)-based method employed by this study uses a series of physical parameters to quantitatively describe the characteristics of urban types, thereby generally ensuring the accuracy of GIS-based mapping results if the parameters are calculated correctly [11]. Additionally, we conducted a correlation analysis between N-LCZ and temperature to evaluate the validity of the N-LCZ classification (Figure 11). The correlation coefficient between the N-LCZ, which incorporates both regional and climatic characteristics, and the microclimate was approximately 0.52. In contrast, the correlation coefficient between LCZ and the microclimate, as shown in Figure 7, was about 0.27. This suggests that the new microclimate urban type-classification system, N-LCZ, has a stronger correlation with the microclimate.

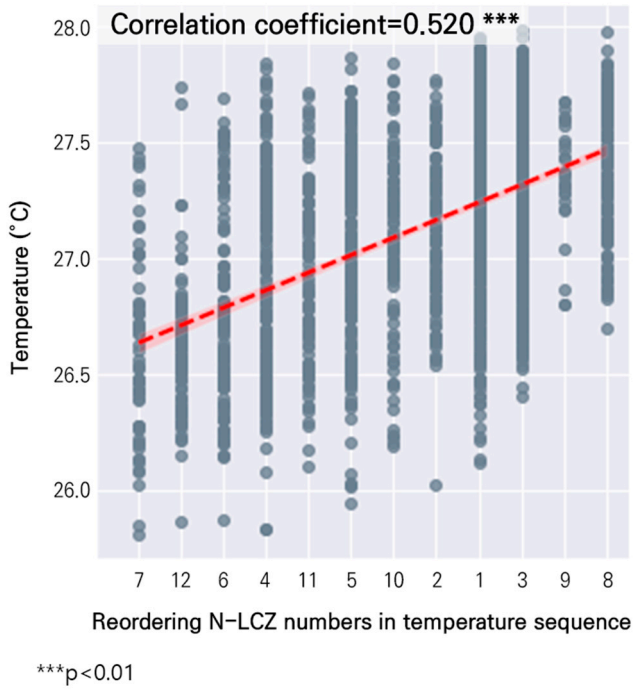

Figure 11. Correlation analysis between new local climate zones and microclimate.

5. Discussion

5.1. Consistency between Urban Type Attributes and Spatial Distribution

This study meticulously examined the LCZ concept, which has been frequently used in UHI-related research, identified its limitations, and developed the highly reliable N-LCZ as a new urban typology-classification system based on microclimate. This study supports subsequent research on UHI and urban thermal environments. From previous research findings, we observed discrepancies between the attributes defined by LCZ and their actual spatial distribution characteristics. For instance, LCZ1, which is typically characterized by densely located high-rise buildings, was observed to classify certain areas in Yeoksam-dong and Gangnam-gu, characterized by densely packed low-rise buildings, as LCZ1. Additionally, land-cover types (LCZA-G) defined as areas devoid of human activity were observed in locations with dense population density such as around the express bus terminal station in Seocho-gu and its vicinity, as well as apartment complexes. The actual correlation between LCZ and microclimate was found to be weak.

Conversely, the newly developed N-LCZ in this study, which takes into account both urban environmental and metabolic factors, has shown a close alignment between the statistical values and spatial distribution characteristics for each type. Moreover, its correlation with microclimates improved by approximately 15% compared to LCZ. We attribute the low correlation between LCZ and microclimate to the fact that type values defined by the existing LCZ theory may not adequately reflect the complex interactions between urban factors contributing to UHI [34]. Previous LCZ types exhibited uniform patterns of increase or decrease in attribute values [7]. In contrast, as shown in Figure 8, the attribute values of the N-LCZ types do not uniformly increase or decrease but instead exhibit distinct characteristics. A cluster can be considered a distinct category if it displays clear features in specific variables even if there is some overlap with other clusters, and the criterion for effective segmentation is the internal validity of the clusters [59,60]. In this respect, N-LCZ represents a system that better reflects the complex outcomes of modern urban interactions than the uniform pattern of increase or decrease typical of urban types.

5.2. The Significance of Urban Metabolism

Secondly, it is deemed crucial to consider human activities, i.e., urban metabolism, in studies on UHI and urban thermal environments. The existing LCZ theory aimed to classify urban types based on surface structure, cover, fabric, and human activity variables that influence microclimate. However, in practice, the focus was predominantly on variables related to surface structure and surface cover. In other words, human activity was not actively incorporated into the LCZ system, and explanations regarding human activity-related variables were insufficient, leading to inadequate consideration in subsequent research endeavors [35,36]. Therefore, this study categorized population density, traffic volume, and electricity energy consumption related to human activity as urban metabolic factors and utilized them in the development of N-LCZ.

N-LCZ types with higher urban metabolic factors generally had higher average temperatures, while types with lower urban metabolic factors had lower average temperatures. For example, N-LCZ8, which had the highest average temperature, also had the highest population density and traffic volume among all types. Furthermore, N-LCZ3 is characterized by moderate to low traffic volume and electricity consumption, yet it boasts the second-highest population density among all types. This aligns with previous findings, which suggest that areas with high human activity and traffic can experience more severe thermal environments [41]. Conversely, N-LCZ2, while having a relatively lower population density compared to N-LCZ8 and N-LCZ3, exhibits the highest electricity consumption of all types. This type recorded the fifth-highest temperature overall. This supports the results from previous studies, indicating that heat emitted from energy usage can significantly impact the urban thermal environment [43]. This correlation suggests that urban metabolism may influence the average temperature of N-LCZ types, and it could

be argued that it should be prominently addressed in future research on UHI and urban thermal environments.

5.3. Microscale Analysis of Urban Thermal Environments

We employed NSV imagery and semantic segmentation techniques to microscopically quantify urban environmental factors such as SVF and GVF. Subsequent analysis revealed that N-LCZ7 and N-LCZ11 share similar attributes across variables, with GVF being the only distinctly differing factor. NSV quantifies vertical greenery at the pedestrian level, so GVF offers a measure of greenery from a different dimension compared to two-dimensional assessments [61]. Observing their spatial distribution, N-LCZ7 was predominantly located around mountainous areas, whereas N-LCZ11 was found not only around mountainous areas but also in surrounding areas and urban parks. This discovery indicates that GVF, a variable that quantifies the vertical aspect of greenery, plays a crucial role in distinguishing between the two distinct clusters. Furthermore, the substantial impact of GVF alone on microclimate variation suggests the necessity of a comprehensive analysis considering the vertical aspect of urban environments.

Given the ambiguity of boundaries between temperature, environmental factors, and socio-economic factors within modern cities compared to the past, research on UHI and urban heat environments is recommended to be conducted at a horizontal, microscale level. Furthermore, the recent concept of UHI resembles an 'archipelago', a more localized range, rather than an 'island', defined by the temperature differences between urban and rural areas, thus necessitating the identification of microscale hotspots and cold spots [62,63]. LCZ, as its name suggests, defined the concept based on a microscale criterion. However, in reality, temperature surveys were conducted that could not adequately represent microclimates, and the analysis unit used for quantifying variables for classification was not specified. We utilized densely arranged S-DoT to investigate urban microclimates and established analysis grids that can be considered microscale based on the spatial autocorrelation of building heights. The research findings revealed that N-LCZ7 and N-LCZ11 had similar attribute values for variables and were spatially close, yet exhibited significant temperature differences. Conversely, N-LCZ2 and N-LCZ10 had completely different attribute values and were physically distant, yet showed relatively small temperature differences. Such statistical and spatial differences may not be adequately captured in horizontally macroscopic analyses, indicating the need for research on microclimates based on sufficiently micro-horizontal scales.

5.4. Limitations of This Study and Further Research

Despite providing a critical review of existing theories and offering significant analytical results and implications, this study has several limitations. Firstly, the definition and data description of surface admittance are insufficient, resulting in a lack of clear criteria for defining this variable [7], which was consequently not addressed in this study. Secondly, while this study used dendrogram analysis to determine the optimal number of N-LCZ types, future research should consider decision-making methods that minimize subjectivity. Thirdly, the choice of a reasonable basic spatial unit may vary depending on the spatial and temporal scope, thus additional analyses in other cities worldwide are necessary. Moreover, to generalize the findings, further empirical studies in various regions are needed. Lastly, due to data availability constraints, the analysis was limited to the summer of 2021. Future research should incorporate a more extensive time series dataset to enhance generalizability.

6. Conclusions

The objective of proposing the LCZ system as a climate-based urban typology framework was to provide an objective framework for UHI research and standardize global UHI observations. However, this theory still has limitations in regional and climatological aspects. Therefore, this study developed a new microclimate-based urban typology-

classification system that incorporates both regional and climatological significance. We aim to support subsequent UHI-related research by providing a specific and reliable framework.

The spatial scope of this study is Seoul, and the temporal scope is set from June to August 2021, covering the summer season. The analysis unit of this study, which serves as the basic spatial unit for N-LCZ, was determined as a 500 m × 500 m grid based on the spatial autocorrelation of building heights using a semi-variogram model. S-DoT temperature data were collected for microclimate investigation in Seoul, enabling spatiotemporal microscale temperature observations. Subsequently, we created an LCZ-classification map of Seoul and investigated the validity of the classification map by comparing the spatial distribution characteristics and original definitions of each type. Following this, correlation analysis between LCZ types and microclimate was conducted, revealing a weak correlation. Thus, based on prior research, this study selected urban environmental and metabolic factors to develop N-LCZ. In particular, we utilized NSV and semantic segmentation techniques to quantitatively analyze not only microclimate, but also urban environmental factors close to the pedestrian level. Hierarchical clustering was performed based on these variables, resulting in the classification of N-LCZ into 12 types. We then conducted an analysis of descriptive statistics and spatial distribution characteristics for each type, performing initial validation of N-LCZ's effectiveness. Subsequently, a second validation was performed through correlation analysis between N-LCZ and microclimate. Ultimately, we concluded that the validity of N-LCZ is higher than that of LCZ and summarized the implications of N-LCZ accordingly.

Author Contributions: Conceptualization, S.P. and S.L.; Methodology, S.P. and S.L.; Software, S.P.; Validation, K.O.; Data curation, S.P.; Writing—original draft, S.P.; Writing—review & editing, S.P., S.L. and K.O.; Visualization, S.P.; Supervision, S.L. All authors have read and agreed to the published version of the manuscript.

Funding: This work was supported by Korea Environment Industry &Technology Institute (KEITI) through "Climate Change R&D Project for New Climate Regime", funded by Korea Ministry of Environment (MOE) (2022003570004).

Data Availability Statement: The original contributions presented in the study are included in the article, further inquiries can be directed to the corresponding author.

Conflicts of Interest: The authors declare no conflict of interest.

Appendix A

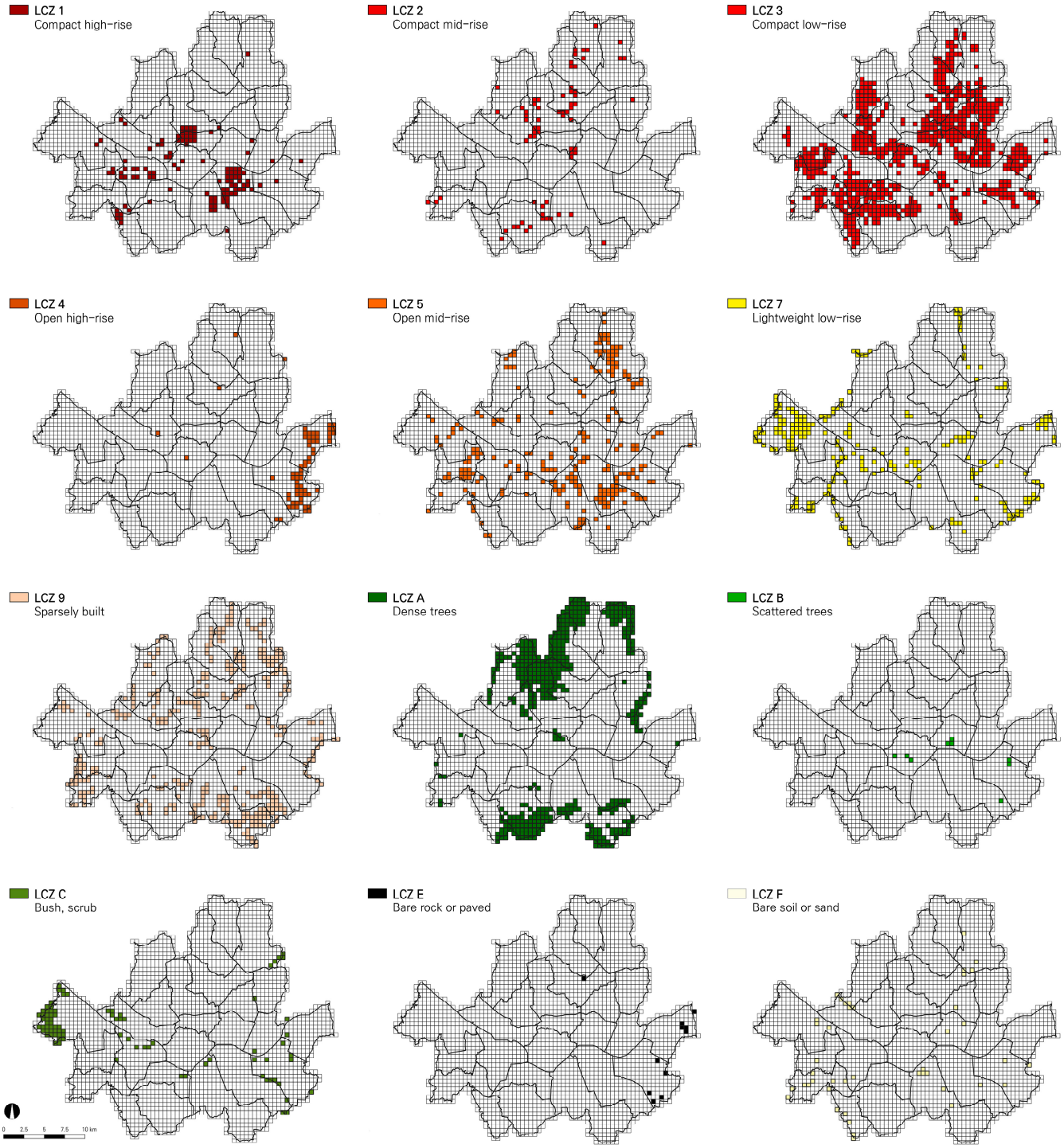

Figure A1. Spatial distribution maps of LCZ types in Seoul.

Appendix B

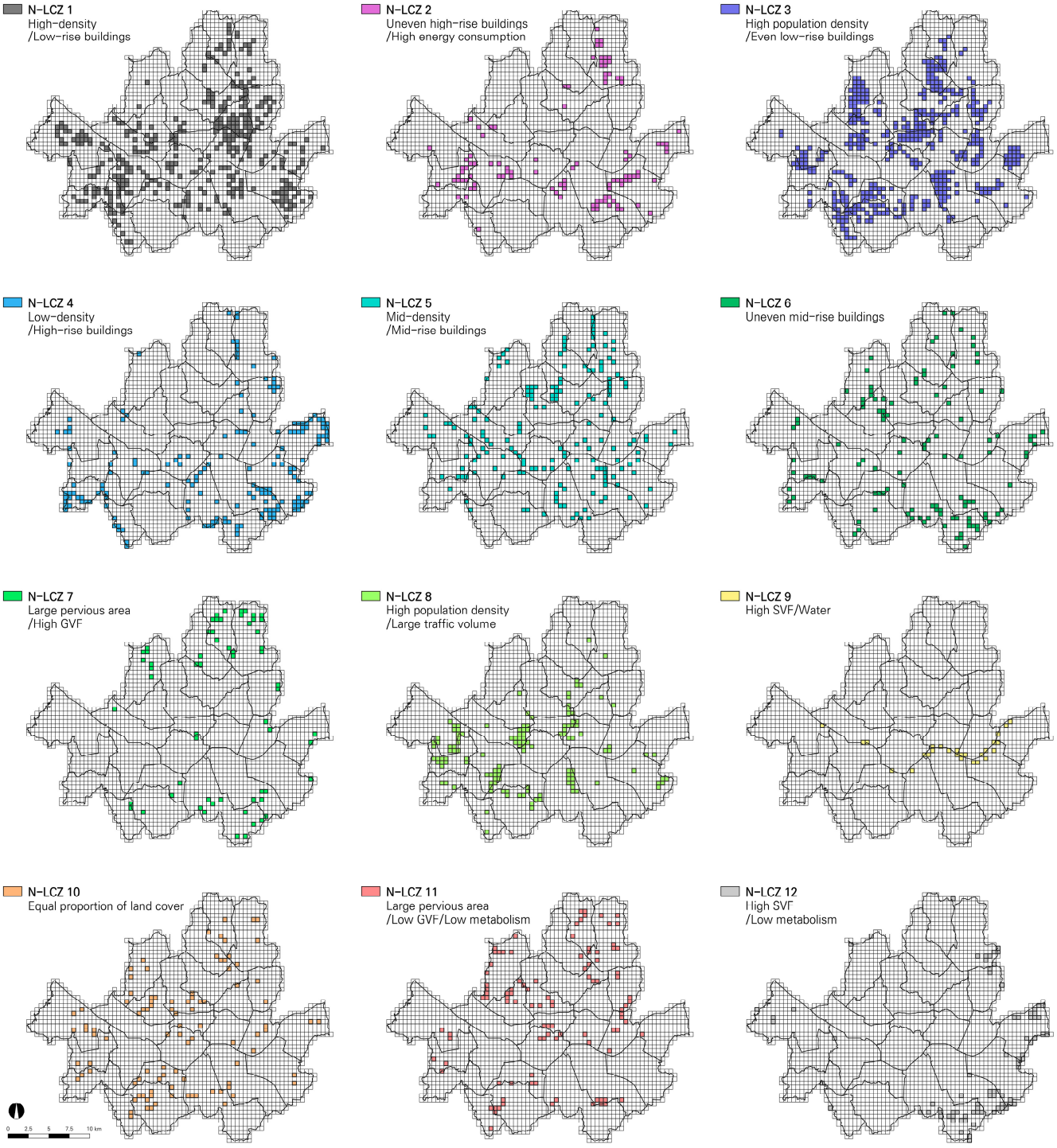

Figure A2. Spatial distribution maps of N-LCZ types in Seoul.

References

1. Zhou, X.; Chen, H. Impact of urbanization-related land use land cover changes and urban morphology changes on the urban heat island phenomenon. *Sci. Total Environ.* **2018**, *635*, 1467–1476. [CrossRef] [PubMed]
2. Oh, K.; Hong, J. The relationship between urban spatial elements and the urban heat island effect. *J. Urban Des. Inst. Korea* **2005**, *6*, 47–63.
3. Monteiro, A.; Ankrah, J.; Madureira, H.; Pacheco, M.O. Climate risk mitigation and adaptation concerns in urban areas: A systematic review of the impact of IPCC assessment reports. *Climate* **2022**, *10*, 115. [CrossRef]

4. Cha, S.; Oh, K. The Impact of the Geometry of Urban Residential Street Canyons on Thermal Comfort-Based on a Decision Tree Analysis Method. *J. Archit. Inst. Korea* **2020**, *36*, 187–198.
5. Ngarambe, J.; Oh, J.W.; Su, M.A.; Santamouris, M.; Yun, G.Y. Influences of wind speed, sky conditions, land use and land cover characteristics on the magnitude of the urban heat island in Seoul: An exploratory analysis. *Sustain. Cities Soc.* **2021**, *71*, 102953. [CrossRef]
6. Cui, D.; Liang, S.; Wang, D. Observed and projected changes in global climate zones based on Köppen climate classification. *Wiley Interdiscip. Rev. Clim. Chang.* **2021**, *12*, e701. [CrossRef]
7. Stewart, I.D.; Oke, T.R. Local climate zones for urban temperature studies. *Bull. Am. Meteorol. Soc.* **2012**, *93*, 1879–1900. [CrossRef]
8. Quan, S.J.; Bansal, P. A systematic review of GIS-based local climate zone mapping studies. *Build. Environ.* **2021**, *196*, 107791. [CrossRef]
9. Brousse, O.; Georganos, S.; Demuzere, M.; Vanhuysse, S.; Wouters, H.; Wolff, E.; Linard, C.; Lipzig, N.; Dujardin, S. Using local climate zones in Sub-Saharan Africa to tackle urban health issues. *Urban Clim.* **2019**, *27*, 227–242. [CrossRef]
10. Chen, Y.C.; Lo, T.W.; Shih, W.Y.; Lin, T.P. Interpreting air temperature generated from urban climatic map by urban morphology in Taipei. *Theor. Appl. Climatol.* **2019**, *137*, 2657–2662. [CrossRef]
11. Huang, F.; Jiang, S.; Zhan, W.; Bechtel, B.; Liu, Z.; Demuzere, M.; Huang, Y.; Xu, Y.; Ma, L.; Xia, W.; et al. Mapping local climate zones for cities: A large review. *Remote Sens. Environ.* **2023**, *292*, 113573. [CrossRef]
12. Xie, J.; Zhou, S.; Chung, L.C.H.; Chan, T.O. Evaluating land-surface warming and cooling environments across urban–rural local climate zone gradients in subtropical megacities. *Build. Environ.* **2024**, *251*, 111232. [CrossRef]
13. Lyu, T.; Buccolieri, R.; Gao, Z. A numerical study on the correlation between sky view factor and summer microclimate of local climate zones. *Atmosphere* **2019**, *10*, 438. [CrossRef]
14. Oke, T.R. Street design and urban canopy layer climate. *Energy Build.* **1988**, *11*, 103–113. [CrossRef]
15. Lin, P.; Gou, Z.; Lau, S.S.Y.; Qin, H. The impact of urban design descriptors on outdoor thermal environment: A literature review. *Energies* **2017**, *10*, 2151. [CrossRef]
16. Houet, T.; Pigeon, G. Mapping urban climate zones and quantifying climate behaviors–an application on Toulouse urban area (France). *Environ. Pollut.* **2011**, *159*, 2180–2192. [CrossRef] [PubMed]
17. Javanroodi, K.; Perera, A.T.D.; Hong, T.; Nik, V.M. Designing climate resilient energy systems in complex urban areas considering urban morphology: A technical review. *Adv. Appl. Energy* **2023**, *12*, 100155. [CrossRef]
18. Hou, H.; Su, H.; Yao, C.; Wang, Z.H. Spatiotemporal patterns of the impact of surface roughness and morphology on urban heat island. *Sustain. Cities Soc.* **2023**, *92*, 104513. [CrossRef]
19. Davenport, A.G.; Grimmond, C.S.B.; Oke, T.R.; Wieringa, J. Estimating the roughness of cities and sheltered country. In Proceedings of the Preprints, 12th Conference on Applied Climatology, Asheville, NC, USA, 8–11 May 2000; American Meteorological Society: Boston, MA, USA, 2000; pp. 96–99.
20. Ng, E.; Yuan, C.; Chen, L.; Ren, C.; Fung, J.C. Improving the wind environment in high-density cities by understanding urban morphology and surface roughness: A study in Hong Kong. *Landsc. Urban Plan.* **2011**, *101*, 59–74. [CrossRef]
21. Leconte, F.; Bouyer, J.; Claverie, R.; Pétrissans, M. Using Local Climate Zone scheme for UHI assessment: Evaluation of the method using mobile measurements. *Build. Environ.* **2015**, *83*, 39–49. [CrossRef]
22. Rodler, A.; Leduc, T. Local climate zone approach on local and micro scales: Dividing the urban open space. *Urban Clim.* **2019**, *28*, 100457. [CrossRef]
23. Yan, J.; Chen, W.Y.; Zhang, Z.; Zhao, W.; Liu, M.; Yin, S. Mitigating PM2.5 exposure with vegetation barrier and building designs in urban open-road environments based on numerical simulations. *Landsc. Urban Plan.* **2024**, *241*, 104918. [CrossRef]
24. Zhang, J.; Li, Z.; Wei, Y.; Hu, D. The impact of the building morphology on microclimate and thermal comfort-a case study in Beijing. *Build. Environ.* **2022**, *223*, 109469. [CrossRef]
25. Zhou, W.; Yu, W.; Zhang, Z.; Cao, W.; Wu, T. How can urban green spaces be planned to mitigate urban heat island effect under different climatic backgrounds? A threshold-based perspective. *Sci. Total Environ.* **2023**, *890*, 164422. [CrossRef] [PubMed]
26. Robitu, M.; Musy, M.; Inard, C.; Groleau, D. Modeling the influence of vegetation and water pond on urban microclimate. *Sol. Energy* **2006**, *80*, 435–447. [CrossRef]
27. Wimberly, M.C.; Davis, J.K.; Evans, M.V.; Hess, A.; Newberry, P.M.; Solano-Asamoah, N.; Murdock, C.C. Land cover affects microclimate and temperature suitability for arbovirus transmission in an urban landscape. *PLoS Neglected Trop. Dis.* **2020**, *14*, e0008614. [CrossRef]
28. Zhang, Y.; Harris, A.; Balzter, H. Characterizing fractional vegetation cover and land surface temperature based on sub-pixel fractional impervious surfaces from Landsat TM/ETM+. *Int. J. Remote Sens.* **2015**, *36*, 4213–4232. [CrossRef]
29. Khamchiangta, D.; Dhakal, S. Physical and non-physical factors driving urban heat island: Case of Bangkok Metropolitan Administration, Thailand. *J. Environ. Manag.* **2019**, *248*, 109285. [CrossRef]
30. Du, P.; Chen, J.; Bai, X.; Han, W. Understanding the seasonal variations of land surface temperature in Nanjing urban area based on local climate zone. *Urban Clim.* **2020**, *33*, 100657. [CrossRef]
31. Yu, W.; Yang, J.; Wu, F.; He, B.; Yu, H.; Ren, J.; Xiao, X.; Xia, J.C. Downscaling mapping method for local climate zones from the perspective of deep learning. *Urban Clim.* **2023**, *49*, 101500. [CrossRef]
32. Dutta, K.; Basu, D.; Agrawal, S. Evaluation of seasonal variability in magnitude of urban heat islands using local climate zone classification and surface albedo. *Int. J. Environ. Sci. Technol.* **2022**, *19*, 8677–8698. [CrossRef]

33. Yang, J.; Wang, Z.H.; Kaloush, K.E. Environmental impacts of reflective materials: Is high albedo a 'silver bullet' for mitigating urban heat island? *Renew. Sustain. Energy Rev.* **2015**, *47*, 830–843. [CrossRef]
34. Ryu, Y.H.; Baik, J.J. Quantitative analysis of factors contributing to urban heat island intensity. *J. Appl. Meteorol. Climatol.* **2012**, *51*, 842–854. [CrossRef]
35. Chen, Y.; Zheng, B.; Hu, Y. Mapping local climate zones using ArcGIS-based method and exploring land surface temperature characteristics in Chenzhou, China. *Sustainability.* **2020**, *12*, 2974. [CrossRef]
36. Hidalgo, J.; Dumas, G.; Masson, V.; Petit, G.; Bechtel, B.; Bocher, E.; Foley, M.; Schoetter, R.; Mills, G. Comparison between local climate zones maps derived from administrative datasets and satellite observations. *Urban Clim.* **2019**, *27*, 64–89. [CrossRef]
37. Fan, P.Y.; He, Q.; Tao, Y.Z. Identifying research progress, focuses, and prospects of local climate zone (LCZ) using bibliometrics and critical reviews. *Heliyon* **2023**, *9*, e14067. [CrossRef] [PubMed]
38. Wolman, A. The metabolism of cities. *Sci. Am.* **1965**, *213*, 178–193. [CrossRef]
39. Zhang, Y. Urban metabolism: A review of research methodologies. *Environ. Pollut.* **2013**, *178*, 463–473. [CrossRef]
40. Currie, P.K.; Musango, J.K.; May, N.D. Urban metabolism: A review with reference to Cape Town. *Cities* **2017**, *70*, 91–110. [CrossRef]
41. Wong, P.P.Y.; Lai, P.C.; Low, C.T.; Chen, S.; Hart, M. The impact of environmental and human factors on urban heat and microclimate variability. *Build. Environ.* **2016**, *95*, 199–208. [CrossRef]
42. Barles, S. Society, energy and materials: The contribution of urban metabolism studies to sustainable urban development issues. *J. Environ. Plan. Manag.* **2010**, *53*, 439–455. [CrossRef]
43. Liao, W.; Liu, X.; Wang, D.; Sheng, Y. The impact of energy consumption on the surface urban heat island in China's 32 major cities. *Remote Sens.* **2017**, *9*, 250. [CrossRef]
44. Li, N.; Quan, S.J. Identifying urban form typologies in Seoul using a new Gaussian mixture model-based clustering framework. *Environ. Plan. B Urban Anal. City Sci.* **2023**, *50*, 2333–2620. [CrossRef]
45. Zheng, Y.; Ren, C.; Xu, Y.; Wang, R.; Ho, J.; Lau, K.; Ng, E. GIS-based mapping of Local Climate Zone in the high-density city of Hong Kong. *Urban Clim.* **2018**, *24*, 419–448. [CrossRef]
46. Kim, J.; Kang, M. A study on the micro-scale heat wave vulnerability assessment using urban data sensors (S-DoT) in Seoul. *J. Korea Plan. Assoc.* **2022**, *57*, 215–234. [CrossRef]
47. Demuzere, M.; Kittner, J.; Bechtel, B. LCZ Generator: A web application to create Local Climate Zone maps. *Front. Environ. Sci.* **2021**, *9*, 637455. [CrossRef]
48. Biswas, G.; Roy, T.K. Measuring Objective Walkability from Pedestrian-Level Visual Perception Using Machine Learning and GSV in Khulna, Bangladesh. *Geomat. Environ. Eng.* **2023**, *17*, 5–27. [CrossRef]
49. Xia, Y.; Yabuki, N.; Fukuda, T. Sky view factor estimation from street view images based on semantic segmentation. *Urban Clim.* **2021**, *40*, 100999. [CrossRef]
50. Nassar, A.; Blackburn, G.; Whyatt, J. Dynamics and controls of urban heat sink and island phenomena in a desert city: Development of a local climate zone scheme using remotely-sensed inputs. *Int. J. Appl. Earth Obs. Geoinf.* **2016**, *51*, 76–90. [CrossRef]
51. Wu, J.; Liu, C.; Wang, H. Analysis of Spatio-temporal patterns and related factors of thermal comfort in subtropical coastal cities based on local climate zones. *Build. Environ.* **2022**, *207*, 108568. [CrossRef]
52. Park, C.; Ha, J.; Lee, S. Association between Three-Dimensional Built Environment and Urban Air Temperature: Focused on Seasonal and Temporal Differences. *Sustainability* **2017**, *9*, 1338. [CrossRef]
53. Murtagh, F.; Contreras, P. Algorithms for hierarchical clustering: An overview. *Wiley Interdiscip. Rev. Data Min. Knowl. Discov.* **2012**, *2*, 86–97. [CrossRef]
54. Liu, N.; Xu, Z.; Zeng, X.J.; Ren, P. An agglomerative hierarchical clustering algorithm for linear ordinal rankings. *Inf. Sci.* **2021**, *557*, 170–193. [CrossRef]
55. Park, N.; Ko, H. Agglomerative hierarchical clustering analysis with deep convolutional autoencoders. *J. Korea Multimed. Soc.* **2020**, *23*, 1–7.
56. Jeong, N.; Lee, J. Hierarchical clustering on international research trends of translation studies-focusing on routledge publications. *J. Humanit. Soc. Sci. 21* **2022**, *13*, 1493–1506. [CrossRef]
57. Yang, J.; Wang, Y.; Xiu, C.; Xiao, X.; Xia, J.; Jin, C. Optimizing local climate zones to mitigate urban heat island effect in human settlements. *J. Clean. Prod.* **2020**, *275*, 123767. [CrossRef]
58. Bechtel, B.; Demuzere, M.; Mills, G.; Zhan, W.; Sismanidis, P.; Small, C.; Voogt, J. SUHI analysis using Local Climate Zones—A comparison of 50 cities. *Urban Clim.* **2019**, *28*, 100451. [CrossRef]
59. Deborah, L.J.; Baskaran, R.; Kannan, A. A survey on internal validity measure for cluster validation. *Int. J. Comput. Sci. Eng. Surv.* **2010**, *1*, 85–102. [CrossRef]
60. Kim, M.; Ramakrishna, R.S. New indices for cluster validity assessment. *Pattern Recognit. Lett.* **2005**, *26*, 2353–2363. [CrossRef]
61. Ki, D.; Lee, S. Analyzing the effects of Green View Index of neighborhood streets on walking time using Google Street View and deep learning. *Landsc. Urban Plan.* **2021**, *205*, 103920. [CrossRef]

62. Buyantuyev, A.; Wu, J. Urban heat islands and landscape heterogeneity: Linking spatiotemporal variations in surface temperatures to land-cover and socioeconomic patterns. *Landsc. Ecol.* **2010**, *25*, 17–33. [CrossRef]
63. Jenerette, G.D.; Harlan, S.L.; Buyantuev, A.; Stefanov, W.L.; Declet-Barreto, J.; Ruddell, B.L.; Myint, S.W.; Kaplan, S.; Li, X. Micro-scale urban surface temperatures are related to land-cover features and residential heat related health impacts in Phoenix, AZ USA. *Landsc. Ecol.* **2016**, *31*, 745–760. [CrossRef]